Published in final edited form as:
J Mol Biol. 2007 November 30; 374(3): 671–687.

EFFECT OF SEQUENCE HYDROPHOBICITY AND BILAYER WIDTH UPON THE MINIMUM LENGTH REQUIRED FOR THE FORMATION OF TRANSMEMBRANE HELICES IN MEMBRANES

Shyam S. Krishnakumar and **Erwin London***
Department of Biochemistry and Cell Biology, Stony Brook University, Stony Brook, NY 11794–5215

SUMMARY

The minimum hydrophobic length necessary to form a transmembrane (TM) helix in membranes was investigated using model membrane-inserted hydrophobic helices. The fluorescence of a Trp at the center of the sequence and its sensitivity to quenching were used to ascertain helix position within the membrane. Peptides with hydrophobic cores composed of polyLeu were compared to sequences containing a poly 1:1 Leu:Ala core (which have a hydrophobicity typical of natural TM helices). Studies varying bilayer width revealed that the polyLeu core peptides predominately formed a TM state when the bilayer width exceeded hydrophobic sequence length by (i.e. when negative mismatch was) up to ~11–12Å (e.g. the case of a 11–12 residue hydrophobic sequence in bilayers with a biologically relevant width, i.e. dioleoylphosphatidylcholine [DOPC] bilayers), while polyLeuAla core peptides formed predominantly TM state with negative mismatch of up to 9Å (a 13 residue hydrophobic sequence in DOPC bilayers). This indicates that minimum length necessary to form a predominating amount of a TM state (minimum TM length) is only modestly hydrophobicity-dependent for the sequences studied here, and a formula that defines the minimum TM length as a function of hydrophobicity for moderately-to-highly hydrophobic sequences was derived. The minimum length to form a stable TM helix for alternating LeuAla sequences, and that for sequences with a Leu block followed by an Ala block, was similar, suggesting that a hydrophobicity gradient along the sequence may not be an important factor in TM stability. TM stability was also similar for sequences flanked by different charged ionizable residues (Lys, His, Asp). However, ionizable flanking residues destabilized the TM configuration much more when charged than when uncharged. The ability of short hydrophobic sequences to form TM helices in membranes in the presence of substantial negative mismatch implies that lipid bilayers have a considerable ability to adjust to negative mismatch, and that short TM helices may be more common than generally believed. Factors that modulate the ability of bilayers to adjust to mismatch may strongly affect the configuration of short hydrophobic helices.

Keywords

membrane proteins; transmembrane helices; minimum transmembrane length; lipid-protein interaction; membrane protein sorting

* Corresponding author: Erwin London, Department of Biochemistry and Cell Biology, Stony Brook University, Stony Brook, NY 11794–5215, Tel: (631) 632–8564, FAX: (631) 632–8875, E-mail: erwin.london@stonybrook.edu.

INTRODUCTION

Transmembrane (TM) segments of membrane proteins are predominantly composed of hydrophobic α-helical segments. Understanding the dependence of hydrophobic helix behavior upon amino acid sequence would vastly improve our ability to predict membrane protein structure, folding and function.

The formation and behavior of short TM helices are poorly characterized. Short TM helices may be more common than generally thought because the length of the TM segment may be smaller than that based on naïve hydrophobicity calculations. In recent work on polio virus 3A/3AB proteins we found the 22-residue hydrophobic anchor of the 3A protein can adopt a TM structure, but the actual length of the TM segment is only about 16 residues[1].

Because short hydrophobic sequences often form TM states with borderline stability[2,3] it is also important to define how sequence controls their equilibration between TM and non-TM states. This equilibrium can often impact membrane-protein function[1,4–11] and genomic analysis suggests that the number of sequences that can undergo TM/non-TM interconversion may be considerable[12].

The behavior of short TM helices is also of interest because of the role of TM helix length in trafficking between membranes. It has been observed that the apparent TM sequences of Golgi proteins are generally shorter (15 residues) than those (18 residues) of plasma membrane proteins[13–15], and a preferential interaction of short TM α-helices with the thinner bilayers of Golgi apparatus is believed to be one mechanism of retention in the Golgi[13–15]. The predicted role of helix length in this type of sorting is supported by studies showing the cellular location of simple TM sequences is a strong function of length[14,16–18].

Artificial hydrophobic α-helices with simple amino acid compositions are useful for further studies of the relationship between helix length and behavior in membranes. Artificial helices have already been widely used to study the sequence-structure relationship in model membranes, and this system has a number of advantages, including the abilities to control environmental factors such as lipid composition and bilayer width and pH (which cannot be controlled in cells and/or detergent-micelle based studies), and the ability to analyze helix behavior with a variety of techniques, including diffraction, NMR, IR and fluorescence spectroscopy[2,15,19–32].

We have developed a set of methods using fluorescence properties to define the topographical states of membrane-inserted hydrophobic α-helices containing a single Trp residue in their hydrophobic core as a function of sequence and bilayer width[1,2,19–22,33–35]. In a previous study using helix-forming Lys-flanked hydrophobic sequences, we found that in DOPC bilayers 15 residue-long polyLeu type sequences result in stable TM insertion, but that the TM configuration is not very stable when the polyLeu sequence is 11 residues long[2]. We also found that polyLeu sequences containing internal charged residues may form truncated TM segments with as little as 11 consecutive hydrophobic residues[19,34].

However, these studies did not define the minimum length capable of forming a stable TM helix for sequences with more biologically relevant hydrophobicities, or how TM stability would be affected by the identity and charge of hydrophilic residues surrounding the hydrophobic sequence. Defining the importance of these parameters was the aim of the present study. Sequences containing polyLeu or polyLeuAla hydrophobic cores of varying lengths, and sequences with various hydrophilic residues flanking the hydrophobic core, were used to precisely define the minimum length required to form a stable TM helix and its dependence upon sequence and environment. We found that even moderately hydrophobic sequences can form autonomous short TM segments under conditions of considerable negative mismatch,

and that the extent to which a TM configuration is formed can be controlled by physiologically relevant changes in bilayer width and pH. This information should aid the prediction of short TM helices from sequence data, and their behavior in different membranes.

RESULTS

Using Fluorescence Emission λmax, Fluorescence Quenching, and Bilayer Width Variation to Define the Topography of the Membrane-Inserted Hydrophobic Helices

The fluorescence properties of a Trp residue located at the center of the hydrophobic sequence was used to define the topography of membrane-inserted peptides[2,22]. When such a peptide adopts a TM orientation this Trp locates at or near the bilayer center, which results in blue-shifted Trp emission λmax (315–320 nm). However, if the peptide adopts a membrane-bound non-TM topography in which the peptide resides close to the bilayer surface, then the Trp locates close to the surface, and the max red shifts, generally to 335–345 nm[2,22]. The exact λmax value in the non-TM state value depends upon how deeply the peptide is buried in the non-TM state, and upon whether in the non-TM state the Trp faces aqueous solution or the bilayer interior[2,22]. Values of λmax in between those for the TM and non-TM state are characteristic of mixtures of TM and non-TM topographies[2,22] or of a shifted TM state wherein only a part of the hydrophobic sequence forms the membrane-spanning segment, and so the Trp is shifted to an intermediate depth[19,34]. These alternatives can also be distinguished from each other (see below).

The effect of changing bilayer width (and thus changing the degree of hydrophobic mismatch between bilayer width and hydrophobic helix length) upon Trp depth aids the characterization of topography, and can help define the length of a TM helix (Figure 1)[2,19,22,34]. [Lipids with monounsaturated acyl chains are used in these studies so that the bilayers remain in the fluid Ld state at room temperature.] Several studies have shown that for a Trp at the center of a hydrophobic sequence fluorescence is generally most blue-shifted when a hydrophobic peptide is incorporated into widest bilayer in which the TM configuration is stable[2,19,22,34]. As a result, the bilayer width at which fluorescence is most blue-shifted distinguishes short, medium and long TM helices (see Figure 1). As bilayer width is further increased, so that *negative* mismatch between helix length and bilayer width develops, Trp λmax red shifts due to the peptide forming an increasing amount of the non-TM state[2,22]. When the TM state is fully lost, the red shift reaches a limiting value. This point can usually only be detected for short and medium length TM helices (Figure 1).

When bilayer width is decreased from the maximum width at which the TM configuration is stable (i.e., in conditions of *positive* mismatch between helix length and bilayer width) there is also a red shift, although generally smaller than that under conditions of negative mismatch[2,22]. This positive mismatch-induced red shift arises from the fact that a Trp at the bilayer center automatically is located closer to the surface as bilayer width decreases, combined with effects due to promotion of (weak) oligomerization by conditions of positive mismatch[2,21,22]. [It appears that the fluorescence of a Trp at the center of the bilayer is more red-shifted when buried in an oligomer than when exposed to lipid[20,21].] When a membrane-bound helix does not form a TM state, but instead sits near or at the surface of the bilayer in non-TM form, a Trp at the center of the sequence shows highly red-shifted fluorescence that is not sensitive to bilayer width (upper line in Figure 1).

Interpretation of λmax results is aided by combining them with more direct measurements of Trp depth. To do this, a dual fluorescence quenching method can be used. This method utilizes two quenchers of Trp fluorescence, acrylamide and 10-DN. Acrylamide (although membrane permeable)[33] resides primarily in the aqueous solution and preferentially quenches the fluorescence of Trp residues near the membrane surface, while 10-DN, a membrane-inserted

quencher, preferentially quenches the fluorescence of Trp buried in the membrane bilayer[33]. The ratio of acrylamide quenching to 10-DN quenching (Q-ratio) responds nearly linearly to Trp depth in the bilayer, with a low quenching ratio (< 0.2) indicating a deeply located Trp near the center of the bilayer, while a high Q-ratio (1.0–3.0) is usually indicative of a Trp near the bilayer surface[33].

Intermediate Q-ratios can arise either from peptides adopting a mixture of conformations with shallow and deep Trp depths, or from peptides that adopt a "single" shifted TM conformation with an intermediate Trp depth. These two alternatives can be resolved by measurement of quencher-induced shifts in Trp λmax[19,33,34]. If a membrane-inserted peptide forms co-existing deep and shallow conformations, then its Trp emission will be composite of red-shifted and blue-shifted emission spectra. In such samples, acrylamide will preferentially quench the shallow Trp, inducing a blue shift in λmax. Conversely, 10-DN will preferentially quench the deep Trp, and induce red shifts. The difference in λmax in the presence of acrylamide and 10-DN, which depends on the amount of each population present, can be up to 15 nm[33,34]. If only a single Trp depth population is present, the difference in λmax in the presence of acrylamide and 10-DN is very small (0–2 nm)[33,34].

Effect of Helix Length and Sequence upon Topography of Membrane-Inserted Short Hydrophobic Helices: 17 Hydrophobic Residues

Using these methods, peptides with short hydrophobic sequences (13–17 residues) were studied in order to determine the minimum length hydrophobic sequence forming stable TM helices (Table 1). PolyLeu (pL)-type sequences were compared to two different types of polyLeuAla (pLA)-type sequences. The first type had alternating Leu and Ala residues, and the second had a block of Leu residues followed by a block of Ala residues. All sequences had a Trp in the center of the hydrophobic sequence to probe helix position within the bilayer. The also had two flanking ionizable residues, Lys unless otherwise noted, at both the N and C-termini of the hydrophobic core sequence.

Figure 2 shows the effect of bilayer width on Trp emission λmax for pL and pLA peptides at pH 7.0. For sequences with [including the Trp] 17 hydrophobic residues (pL_{16}, $p(LA)_8$ and pL_8A_8), the pattern of λmax as a function of bilayer width (Figure 2A) showed a minimum with very blue-shifted emission in DOPC vesicles (DOPC has 18 carbon acyl chains) and/or dieicosenoylphosphatidylcholine [DEiPC] vesicles (DEiPC has 20 carbon acyl chains) and a significant red shift in wider bilayers. This pattern indicated that in DOPC vesicles the Trp is near the bilayer center, and thus the 17 hydrophobic residue sequences were forming relatively stable TM helices in DOPC vesicles, but in much wider bilayers the Trp located more shallowly, consistent with some degree of formation of a non-TM state.

These conclusions are confirmed by fluorescence quenching data (Figure 3, individual quenching values for acrylamide and 10-DN are given in Supplemental Table 1). All three peptides with 17 hydrophobic residues exhibited low Q-ratios in DOPC vesicles (Figure 3A) corresponding to either fully or almost fully TM configurations with the Trp near the bilayer center, and higher Q-ratios (Figure 3B) in dierucoylphosphatidylcholine [DEuPC] vesicles (DEuPC has 22 carbon acyl chains) indicating a shallower Trp depth that corresponds to some degree of formation of a shallow, non-TM state with the Trp closer to the bilayer surface.

The λmax values in Figure 2A also show that the $p(LA)_8$ and pL_8A_8 give significantly more red-shifted fluorescence than pL_{16} at all bilayer widths, strongly suggesting that the Trp in the former peptides located more shallowly than in the latter peptide. This is confirmed by the observation that $p(LA)_8$ and pL_8A_8 exhibited higher Q-ratios than pL_{16} in both DOPC and DEuPC vesicles (Figure 3).

Furthermore, for $p(LA)_8$ and pL_8A_8 the red shift in λmax appears to approach a limiting value as bilayer width is increased (Figure 2A), indicating nearly complete formation of the non-TM state in very wide bilayers, while for the pL_{16} peptide in wide bilayers the Trp remains relatively blue-shifted, indicating that the TM state still predominates. This conclusion is supported by the quenching data in DEuPC vesicles (Figure 3B), which shows high Q-ratios characteristic of a shallow Trp for the former peptides, but a low Q-ratio for pL_{16} indicating that a predominant amount pL_{16} remained in the TM state, in which Trp locates very deeply.

The differences between λmax and Trp depths for pL_{16} and the $p(LA)_8$ and pL_8A_8 peptides incorporated into moderate-width (DOPC) and even thinner bilayers may result from the TM configuration being less stable for the latter two peptides. However, it is also possible that part of the difference between can be explained by the $p(LA)_8$ and pL_8A_8 peptides forming a TM state with a wider distribution of Trp depths than that of pL_{16} (see Discussion). Consistent with this hypothesis, Table 2 shows that acrylamide and 10-DN do not induce large shifts in λmax for pLA peptides in DOPC vesicles, indicating that the pLA peptides in DOPC vesicles do *not* form two populations with very different Trp depths (i.e. co-existing TM and non-TM states), despite locating more shallowly than the pL peptide.

Effect of Helix Length and Sequence upon Topography of Membrane-Inserted Short Hydrophobic Helices: 15 Hydrophobic Residues

Qualitatively, the pattern of both λmax (Figure 2B) and Q-ratios (Figure 3) for sequences with 15 hydrophobic residues (pL_{14}, $p(LA)_7$ and pL_7A_7) was similar to that for sequences with 17 hydrophobic residues. However, sequences with 15 hydrophobic residues exhibited more red-shifted Trp fluorescence (Figure 2B) than sequences with 17 hydrophobic residues (Figure 2A), consistent with the former having less stable TM insertion due to having shorter hydrophobic segments. This conclusion was supported by the observation that the bilayer width at which λmax is a minimum was thinner for pL_{14} (18 acyl chain carbons), than for pL_{16} (20 acyl chain carbon atoms), and the observation that both $p(LA)_7$ and pL_7A_7 showed near-limiting red shifts in bilayers with 20 acyl chain carbon atoms while $p(LA)_8$ and pL_8A_8 only showed near-limiting red shifts in wider bilayers with 22 acyl chain carbon atoms. Quenching ratios confirmed this difference between 15- and 17- hydrophobic residue sequences. In DOPC vesicles (Figure 3A), the Q-ratios are slightly higher, and thus Trp depth was slightly shallower, for the peptides with 15 hydrophobic residues than it was for the corresponding peptides with 17 hydrophobic residues. The less stable TM insertion of the 15 hydrophobic residue peptides was also confirmed by quencher-induced λmax shifts in DOPC vesicles (Table 2). In contrast to the behavior of $p(LA)_8$ and pL_8A_8, quenching-induced λmax shifts in DOPC vesicles were significant for $p(LA)_7$ and pL_7A_7, indicating that the latter peptides formed significant amounts of both TM and non-TM states in DOPC vesicles, while the former peptides did not (they formed much less non-TM state).

As in the case of the analogous sequences with 17 hydrophobic residues, the pL_{14} peptide showed more blue-shifted fluorescence than the $p(LA)_7$ or pL_7A_7 peptides at all bilayer widths (Figure 2B), indicative of a shallower Trp location for the latter peptides. In agreement with this data, Q-ratios (Figure 3) confirmed that pL_{14} forms structures with a deeper Trp depth than $p(LA)_7$ and pL_7A_7. In addition, in DOPC vesicles the pL_{14} peptide did not show the significant quencher-induced λmax shifts seen with $p(LA)_7$ or pL_7A_7 (Table 2), also consistent with its maintaining a more stable TM configuration (similar to the pL_{16} peptide).

The difference between Q-ratios (and λmax) for $p(LA)_7$ and pL_7A_7 and those for $p(LA)_8$ and pL_8A_8 were not as large in DEuPC vesicles as they were in DOPC vesicles (Figure 2A, 2B,and Figure 3B), probably because in DEuPC vesicles the non-TM state is already predominant in all of these cases. In contrast, Q-ratios and λmax both indicate that in DEuPC vesicles pL_{14} has a shallower Trp depth than pL_{16}. Nevertheless, the TM state appears to predominate for

pL_{14} in DEuPC vesicles as judged by the observation that λmax and Q-ratio values for this peptide in DEuPC vesicles (325 and 0.32, respectively) were closer to the values it exhibited in DOPC vesicles (319 and 0.04, respectively), in which the TM state is formed, than they were to that for pLA_7 and pL_7A_7 peptides in DEuPC vesicles (333–337 nm and 0.88–0.92, respectively), cases in which the peptides appear to be almost fully in the non-TM state.

Effect of Helix Length and Sequence upon Topography of Membrane-Inserted Short Hydrophobic Helices: 13 Hydrophobic Residues

The λmax values for peptides with 13 hydrophobic residues (pL_{12}, $p(LA)_6$ and pL_6A_6) also follow patterns somewhat analogous to that observed for sequences with 15 or 17 hydrophobic residues. However, the peptides with 13 hydrophobic residues exhibited much more red-shifted Trp fluorescence (Figure 2C), than observed for peptides with 15 or 17 hydrophobic residues, and this, plus λmax vs. bilayer width profiles, were indicative of even less stable TM insertion and shorter TM segments than for the peptides with 15 or 17 hydrophobic residues. The latter conclusion is supported by the observation that for all of the peptides with 13 hydrophobic residues the bilayer width at which λmax is a minimum is that of dipalmitoleoylphosphatidylcholine [DPoPC] vesicles (DPoPC has 16 carbon acyl chains), thinner than that giving a minimum λmax for the 15 and 17 hydrophobic residue peptides.

Quenching ratios and quencher-induced λmax shifts again support the conclusions derived from λmax data. In DOPC vesicles, pL_{12}, $p(LA)_6$, and pL_6A_6 show high Q-ratios and large quencher induced λmax shifts, indicating a large amount of the non-TM state is present, (Figure 2C). The lesser stability of the TM state for pL_{12} relative to pL_{14} and pL_{16}, demonstrated by its exhibiting a high Q-ratio (Figure 3A) and large quencher-induced λmax shifts in DOPC vesicles (Table 2), is particularly striking. This difference is confirmed by behavior in DEuPC vesicles, in which pL_{12} differs from pL_{14} and pL_{16} in that it fully forms the non-TM state as judged a very high Q-ratio (Figure 3B).

For all of the peptides with a 13-residue hydrophobic sequence the limiting λmax in wide bilayers was significantly more red-shifted (close to 350 nm) than for 15- and 17-residue long hydrophobic sequences (generally 335–340 nm), indicative of a shallower Trp location in the case of the 13-residue hydrophobic sequences. Consistent with this conclusion, the Q-ratio for the peptides with 13-residue hydrophobic sequences in the non-TM state (~3) was larger than that of the peptides with the 15- and 17-residue hydrophobic sequences in the non-TM state (~1) (Figure 3). This difference could reflect either a shallower peptide location for the 13 residue hydrophobic peptides in the non-TM state or a difference in Trp orientation in the non-TM state (see Discussion). Another possible explanation was that the peptides with 13 hydrophobic residues were not fully membrane-bound. However, control experiments in which vesicles containing pL_6A_6 were chromatographed on Sepharose 4B confirmed that membrane binding was complete (data not shown).

It is noteworthy that although a Q-ratio value of about 1 can represent a fully non-TM configuration, because of the high Q value in the non-TM state for the sequences with 13 hydrophobic residues, the value of about 1 observed for pL_{12}, $p(LA)_6$, and pL_6A_6 in DOPC vesicles is indicative of a mixture of deep and shallow configurations. This is confirmed by the very large quencher-dependent λmax shifts observed for pL_{12}, $p(LA)_6$, and pL_6A_6 in DOPC vesicles (Table 2).

As with the longer peptides, the pL_{12} peptide shows more blue-shifted fluorescence than the $p(LA)_6$ and pL_6A_6 peptides in DOPC vesicles. However, the difference is small, and no difference is detected by Q-ratio, suggesting that the stability of the TM state for the pL_{12} peptide is not much greater than that for $p(LA)_6$ or pL_6A_6.

Secondary Structure of Peptides: Effect of Helix Length and Mismatch

Previous studies have shown the types of peptides studied here form α-helices when membrane-associated[2,36]. To confirm this was true for the specific combinations of sequence and hydrophobic residue lengths studied in this report, the peptides were incorporated into vesicles composed of DOPC or DEuPC and then helix content was estimated from circular dichroism (CD) spectra. Estimated helix contents were found to be in the range of 80–90% (Supplemental Table 2). The results show that the peptides were highly helical in both the TM and non-TM state.

Minimum Length Required for Stable TM Helix Formation

The data from the experiments above was further analyzed to define the sequence/bilayer width dependence of the minimum length required for TM helix formation. To do this, the dependence of Trp λmax upon negative mismatch (the degree to which bilayer width exceeds the length of the hydrophobic sequence) was calculated (Figure 4). The value of λmax was used as a crude measure of the fraction of peptide molecules in the TM configuration, based on the observation that λmax in the TM state falls in the 315–320 nm range, and that for the non-TM state usually falls in the 340–350 nm range. The amount of negative mismatch (in angstroms) was calculated for each peptide/lipid vesicle combination as described in the legend to Figure 4.

Figure 4A shows the behavior of the pL type peptides as a function of negative mismatch, combining the results in this study (triangles) with those of our previous study on pL_{10} and pL_{18} peptides (circles)[2]. The dependence of λmax upon negative mismatch indicates that the TM state for pL sequences is tolerant of up to ~11–12 Å negative mismatch before the non-TM state predominates (Figure 4A). This degree of mismatch would be roughly equivalent to that for an 11–12 residue long hydrophobic sequence in a DOPC bilayer.

It should be noted that there was good agreement between λmax behavior as a function of bilayer width for the pL peptides studied here and those studied previously, with the behavior the pL_{12}, pL_{14} and pL_{16} falling between that previously determined for pL_{10} and pL_{18} (see Figure 1B in Ren et al[2]). [Note the change in nomenclature in this report: in Ren et al[2] the subscript used was larger by one residue because it designated the total number of hydrophobic core residues including the Trp.]

Figure 4B shows that the pattern of λmax vs. negative mismatch for the pLA-type peptides was in general similar to that for the pL-type peptides, with very little difference for the p(LA)n (squares) and pLnAn (diamonds) series. However, the TM configuration for the pLA peptides was more sensitive to mismatch than that for the pL peptides (compare solid and dashed line in Figure 4B). For the pLA peptides the maximum degree of mismatch at which the TM state predominates (i.e. the midpoint of the sigmoidal curve) is about 9Å, which is equivalent to a 13 residue long hydrophobic sequence in a DOPC bilayer. In addition, there seems to be a slightly more gradual dependence of TM stability upon the degree of negative mismatch for the pLA peptides.

It should be noted that vesicle curvature is unlikely to have affected these conclusions. Control experiments using peptides inserted into MLV gave λmax vs. bilayer width results very similar to those obtained with SUV (see Supplemental Figures 1A and 1B). Furthermore, it should be noted that the observed behavior of the peptides represents their equilibrium behavior. Control experiments using membrane-bound decane to reversibly increase bilayer width and alter the TM/non-TM equilibrium[33] demonstrated that (as judged by red-shifted λmax and increased acrylamide quenching) the membrane-inserted state formed by a short hydrophobic peptide (pL_{12}) rapidly and reversibly converted from the TM state to the non-TM configuration when bilayer width was altered *in situ* by decane addition or removal (data not shown).

Effect of Flanking Hydrophilic Residues on the Minimum Length Hydrophobic Sequence Forming a Stable TM Helix

Because the identity of the hydrophilic residues flanking a hydrophobic sequence could influence the effective hydrophobic sequence length, the effect of different ionizable residues flanking the hydrophobic core upon stability of the TM configuration was studied. The behavior of pL_{12} sequences flanked on both on N- and C-termini either by 2 Lys, 1 Lys + 1 His, 2 His, or 1 His + 1 Asp was examined.

Figure 5 shows the dependence of Trp λmax upon bilayer width for these peptides at different pHs. At pH 4.0, where His and Lys both carry positive charge while Asp is largely uncharged (34 and see below), peptides flanked with two Lys-residues ($^{KK}pL_{12}$), 1 Lys + 1His ($^{KH}pL_{12}$) or 2 His ($HHpL_{12}$) showed similar patterns of λmax vs. bilayer width, with fluorescence most blue-shifted for peptide inserted into (16 carbon acyl chain) DPoPC vesicles (Figure 5A). [In this section the designation $^{KK}pL_{12}$ is used for the pL_{12} peptide for clarity.] In addition, in both DOPC and DEuPC bilayers Trp quenching data showed similar Q-ratios for these peptides (Figure 6A). As noted above in the case of $^{KK}pL_{12}$, these λmax and Q-ratio values are indicative of the formation of a mixture of TM and non-TM state in DOPC bilayers, and formation of the non-TM state in wider bilayers. The presence of a mixture of TM and non-TM conformations in DOPC vesicles for these three peptides is confirmed by the observation of large quencher-induced shifts (Table 3). Combined, this data confirms these three peptides have very similar TM stabilities at low pH. At most, $^{KH}pL_{12}$ and $HHpL_{12,}$ gave λmax values in DOPC bilayers that are very slightly more blue-shifted, and Q-ratios slightly lower, than that for $^{KK}pL_{12}$, suggesting slightly more stable TM insertion than for $^{KK}pL_{12}$. These results indicate that the effect of flanking Lys^+ and His^+ residues upon the stability of the TM configuration do not differ greatly. This result is interesting because Lys snorkeling, which is the positioning of the Lys side chain so that its amino charge should be close to the bilayer surface[37], should help stabilize a TM configuration relative to a like-charged residue that cannot snorkel as well (i.e. His)(see Discussion).

Relative to the Lys- and His-flanked peptides at pH 4, the HD-flanked peptide ($^{HD}pL_{12}$) adopted a somewhat more stable TM topography when inserted into DOPC vesicles at pH 4, as judged by its more blue-shifted λmax and lower Q-ratios relative to the other peptides (Figures 5A and 6A, respectively). In fact, for $^{HD}pL_{12}$ in the TM state appears to predominate in DOPC as judged by the lack of strong quencher-induced shifts in λmax (Table 3). The effective length of the TM sequence also appears to be slightly longer than that of the other peptides, as judged by an increase in the acyl chain length at which λmax is at a minimum (Figure 5A). These results reflect the fact that it is easier to place an uncharged Asp near or within the polar/hydrophobic boundary of the bilayer than it is to place a charged residue near this boundary[38].

These experiments were repeated at pH 7 (Figures 5B and 6B) and pH 9 (Figures 5C and 6C). At pH 9 Lys will remain cationic[21], while the other flanking residues should deprotonate, so that His is uncharged and Asp is anionic. Consistent with this, $^{KK}pL_{12}$ did not exhibit any pH-dependence in λmax or Q-ratio, while all the other peptides exhibited a significant pH-dependence in these parameters (compare Figures 5A, 5B, and 5C and Figures 6A, 6B, and 6C). To confirm that there was a change in protonation, the pKa of the flanking residues was determined from the effect of pH upon the fluorescence of the membrane-inserted peptides (Supplemental Figure 2). The lack of charge on His at pH 9 was confirmed by pH dependence of the fluorescence of $^{KH}pL_{12}$ and $^{HH}pL_{12}$ peptides, which indicated an apparent (His) pKa close to pH 7. A pH-dependent change in fluorescence was also observed for the $^{HD}pL_{12}$ peptide, and it appeared that the first (Asp) pKa occurred near pH 5–5.5 and the second (His) pKa near 8. This Asp pKa value is in agreement with previous studies on closely related sequences, which indicate that the pKa for an Asp residue near the end of a hydrophobic

sequence occurs in the range 5–7[34]. In the case of $^{HD}pL_{12}$ His pKa may be increased (relative to the $KHpL_{12}$ and $^{HH}pL_{12}$ peptides) by a favorable interaction between the His and the charged Asp residue.

When λmax (Figure 5C) and Q-ratio (Figure 6C) were measured for membrane-inserted $^{KH}pL_{12}$ and $^{HH}pL_{12}$ at pH 9 (i.e. when the His was uncharged) the values obtained indicated that the peptides had an increased tendency to form the TM state relative to that at pH 4, while for the $^{HD}pL_{12}$ peptide at pH 9 (i.e. when Asp was charged) a decreased tendency to form the TM state was detected relative to that at pH 4.

The stabilization of the TM state at pH 9 in the case of the $^{KH}pL_{12}$ and $^{HH}pL_{12}$ peptides is consistent with the loss at pH 9 of the quencher-induced shifts observed at low pH (Table 3). This indicates that these peptides no longer form a mixture of TM and non-TM states at pH 9. Similarly, the destabilization of the TM state for the $^{HD}pL_{12}$ peptide at pH 9 is consistent with the observation of increased quencher-induced shifts in Trp fluorescence in DOPC vesicles at this pH, indicating formation of co-existing TM and non-TM states (Table 3). These shifts are not seen at pH 4, where the TM state predominates. Thus, comparison of behavior at high and low pH shows that when flanking ionizable residues are charged, they destabilize the TM state to a much greater degree than when they are uncharged, at least for short hydrophobic helices (see Discussion).

At pH 7, λmax (Figure 5B), quenching (Figure 6) and quencher-dependent λmax shift data (Table 3) tended to be intermediate between that at pH 4 and pH 9, with the $^{KH}pL_{12}$ and $^{HH}pL_{12}$ sequences behaving more like they do at pH 9 than at pH 4. The intermediate behavior pattern is consistent with the His, and perhaps Asp, being partially charged at pH 7.

DISCUSSION

The Minimum Length Threshold for Transmembrane Helices: Dependence Upon Bilayer Width and Sequence Hydrophobicity

This study investigated how negative hydrophobic mismatch and sequence combine to affect the relative stability of TM and non-TM configurations of short membrane-inserted hydrophobic helices. The results show that for highly hydrophobic sequences, 11–12 consecutive hydrophobic residues is about the minimum to form a TM configuration sufficiently stable to be the predominant configuration (i.e. 11–12 is the minimum TM length) in a bilayer with a biologically relevant width (i.e. DOPC). Less hydrophobic sequences have to be longer to form a stable TM state. However, the effect of hydrophobicity was relatively modest. For an alternating Leu and Ala sequence, 13 consecutive residues is the minimum necessary to form a predominantly TM state in DOPC vesicles. This sequence is of more biological relevance, because the hydrophobicity of an alternating Leu/Ala sequence is more typical of TM sequences in membrane proteins[12]. By assuming a near-linear relationship between minimum TM length and hydrophobicity, we can derive a formula for estimating minimum TM length for a hydrophobic sequence surrounded by charged residues. Using our TM tendency scale[12] as a measure of hydrophobicity gives the formula:

$$\text{Minimum TM length} = 15.6 - (2.1)(\text{average TM tendency value of core sequence}) \quad \text{Eq. 1}$$

As an alternative, using the biological hydrophobicity scale of Hessa *et al.*[39] gives the formula:

$$\text{Minimum TM length} = 14.3 + (4.5)(\text{average biological hydrophobicity value of core sequence}) \quad \text{Eq. 2}$$

(These equations have been corrected for Trp and Gly residues in our peptides, see below.) Since biological hydrophobicity was derived for residues near the bilayer center, it should be

most accurate equation for synthetic sequences with deep Trp or Tyr residues, such as those used in this study, while TM tendency is more appropriate for natural sequences in which Trp and Tyr are generally located close to the edge of the bilayer.

We do not yet know over how wide a range of sequences these equations are useful. At most, they should only be valid for moderately-to-highly hydrophobic sequences, and they can not be applied to weakly hydrophobic sequences, as illustrated by the relationship of the energetics of TM insertion vs. hydrophobic sequence length, shown schematically in Figure 7. The free energy of burial of hydrophobic residues will basically be proportional to the number of hydrophobic residues multiplied by the average per residue free energy of burial. However, the energetic behavior of the hydrophilic flanking residues is more complex. In the region of negative mismatch, the unfavorable free energy associated with burial of hydrophilic flanking residues (or equivalently, that of any compensating bilayer distortions, see below) should become progressively worse as hydrophobic sequence length decreases. In the region of positive mismatch, there should still be a residual unfavorable free energy associated with locating hydrophilic flanking residues in the polar headgroup region close to the bilayer surface, because the polar headgroup forms a more non-polar environment than aqueous solution, but this free energy should be only weakly dependent on the length of the hydrophobic sequence. The reasons for this are that the polar headgroup region is not highly hydrophobic and any helix tilting to maintain burial of hydrophobic residues under conditions of positive mismatch (see below), will tend to result in a nearly constant headgroup position relative to the bilayer surface (as shown schematically in Figure 7). Because of this, weakly hydrophobic sequences should tend to exhibit a high minimum TM length value that is stongly dependent upon the exact value of sequence hydrophobicity (Figure 7). This sensitivity to hydrophobicity would be somewhat ameliorated if helix tilt is disfavored due to disturbed lipid packing by tilted helices, and/or if there is a strong tendency of weakly hydrophobic residues to protrude into aqueous solution[40].

The weak dependence of minimum TM length upon hydrophobicity for moderately-to-highly hydrophobic sequences means that correcting for the destabilizing effect of the Trp that was placed in the center of the hydrophobic sequences[39] did not significantly modify the value of minimum TM length. Based on the hydrophobicity of Trp[39], the decrease in hydrophobicity due to a Trp should only have increased the effective minimum TM length for our peptides by about 0.2 residues (calculation not shown). Furthermore, this effect is more than cancelled out by the Gly residue that was contiguous to the hydrophobic sequences (Gly was present so that the results could be compared to previous studies[2,22] - the Gly was originally a purity marker for chemical synthesis[41]). Based on the conclusion that a polar residue flanking a hydrophobic sequence increases the effective length of a hydrophobic sequence by about half as much as a non-polar residue (see below), the Gly should have decreased the apparent minimum TM length of the hydrophobic core by ~ ½ residue. Thus, overall the core sequences used in this study should only behave slightly differently than sequences with pure Leu or pure LeuAla hydrophobic cores.

Difference in Energetic Effects of Leu and Ala Upon TM vs. Non-TM Membrane Insertion

Ala is significantly less hydrophobic than Leu, and peptides with hydrophobic cores composed entirely, or almost entirely, of Ala are not stable in the TM state[39,42–44]. This raises the question: what was the loss of TM stability due to Ala in the pLA peptides? Estimating the fraction of peptide molecules in the TM and non-TM configurations state under conditions of 10Å of negative mismatch (the fraction in the non-TM configuration being roughly given by the red shift of λmax at 10Å mismatch relative to λmax at no mismatch divided by the limiting red shift at infinite mismatch relative to that no mismatch, see Figure 4) allows calculation of both an approximate ΔG° for the TM/non-TM equilibrium and a ΔΔG° for the difference in

TM stability between a pL and pLA sequence. [It should be noted that we did not correct average λmax values for the difference in intensity in the TM and non-TM states because we found that the intensity in the non-TM state was only 5–20% less than in the TM state (data not shown).]

This calculation yields an estimate a ΔΔG° of ~0.50 kcal/mole more stable TM insertion for a pL sequence relative to a pLA sequence. For $p(LA)_7$, this would correspond to 0.07 kcal/mole per Leu-to-Ala substitution. However, upon conversion of the TM to non-TM state, Ala at the end of a hydrophobic sequence will not change their membrane depth/exposure to aqueous solution significantly, and of the remaining Ala on the average about half will point towards the center of the bilayer in the non-TM state, and so would not be likely to contribute much to the difference in energy between TM and non-TM states. In the case of $p(LA)_7$ these considerations result in an estimate of 0.2 kcal/mole less stable TM insertion per Leu-to-Ala substitution for residues moving form a deep to shallow location upon conversion of the TM state to the non-TM state.

Even this value is smaller than the ΔΔG° predicted by the biological hydrophobicity scale for a Leu to Ala substitution(0.66 kcal/mole)[39]. In the case of biological hydrophobicity the non-TM state is likely to be the solution state, and it has been found that ΔG^o for partition between aqueous environments and the bilayer surface is about half of the ΔG^o for partition between aqueous to hydrophobic environments[38]. Thus, $\Delta\Delta G^o$ predicted by biological hydrophobicity might be as low as 0.33 kcal/mole. The remaining difference between this value and that we observe (0.2 kcal/mol) may involve the location of our peptides in the non-TM state. Our sequences were much more hydrophobic than those used to estimate energy for peptides at the membrane-solution interface[38], and so our peptides are likely to be located more deeply in the non-TM state, decreasing the difference between free energy in the TM state and surface-bound non-TM state.

The value of $\Delta\Delta G^o$ we obtained should not be over-generalized. First, the number of Leu to Ala substitutions affected by the change from a TM to non-TM state depends on helix length. Second, the accuracy of these calculations is limited by the fact that λmax is not an exact measure of the fraction of peptide in a TM configuration due to factors such as sequence-dependent differences in the λmax of a pure TM form and pure non-TM form. This latter factor certainly is responsible for the scatter in the λmax data in Figure 4 at very high mismatch values. On the other hand, the weighting of average λmax in mixtures of TM and non-TM forms due to conformation-dependent differences in Trp intensity (quantum yield), is not of much concern because the peptides used exhibited only small intensity changes in different configurations (data not shown). In any case, the analysis of λmax shifts provides a useful first estimate of free energy differences.

The Minimum Length Threshold for Transmembrane Helices: Effect of the Hydrophilic Residues Flanking the Hydrophobic Sequence

As noted above, the membrane burial of hydrophilic residues flanking the hydrophobic sequence is likely to be a major factor destabilizing TM insertion of short TM helices. Consistent with this, the experiments in this report demonstrated that when ionizable residues flanking the hydrophobic sequence are charged, they destabilize the TM state to a much greater degree than when they are uncharged. The strongly destabilizing effect of charged flanking residues is not surprising because in the TM state their local environment should be more hydrophobic than in aqueous solution, even if not nearly as hydrophobic as that in the core of the bilayer. However, it was surprising that under conditions in which the flanking residues were charged the His-flanked peptides had a similar TM stability as Lys-flanked peptides. It might be predicted that Lys would be less destabilizing because it has a long side chain and so can position its charged amino group at a much shallower location than the depth of the Lys

backbone (i.e. snorkel)[29]. A possible explanation is that although His cannot snorkel to as great a degree as Lys, its positive charge should be somewhat delocalized, which would reduce destabilization of the TM state.

It was also found that for both $^{KH}pL_{12}$ at high pH and $HDpL_{12}$ at low pH, conditions in which the pLeu sequence is immediately bounded by *uncharged* ionizable residues, the TM state was considerably more stable than at pH values at which these residues were charged. In both these cases, λmax vs. bilayer width profiles and Q-ratio values fell between those of pL_{12} and pL_{14} sequences (compare Figures 2 and 5). Thus, the effective minimum sequence length to form a predominantly TM state was about one residue longer when the two residues flanking the sequence were charged than when they were uncharged. This fits a rule in which the effective minimum TM configuration-forming length equals the number of hydrophobic residues plus about ½ of the number of uncharged hydrophilic residues flanking the hydrophobic core. Studies of sequences in which the identity of the flanking uncharged hydrophilic residues are varied will be required to confirm and refine this conclusion.

Insights into the Details of TM and Non-TM Topographies From Trp Depth

It should be noted that the depth of Trp in membranes is affected by factors in addition to whether sequences are TM or non-TM. Peptide orientation in the shallow, non-TM state is one such factor, as we found previously for longer helices[34]. In the non-TM state, membrane-bound helices orient to place their more polar face towards the aqueous solution. Helical wheel representations of the sequences used in this study (not shown), indicate that for the 13 hydrophobic residue sequences, Lys and Trp are aligned on one helix face to a greater degree than for the other length sequences studied. If the Lys-containing face points toward the aqueous solution, the Trp would also do so, and this would explain why the non-TM state for the 13 hydrophobic residue sequences gave a more red-shifted λmax and higher Q-ratio than the other sequences.

A factor that may affect Trp depth in the TM state is how firmly a TM state is anchored in a specific position. A peptide forming a TM state with ends that are not tightly anchored at the bilayer surface might be able to undergo considerable movement perpendicular to the plane of the membrane, allowing formation of a distribution of TM structures in which the Trp is not always located exactly at the center of the bilayer even though the Trp is in the center of the hydrophobic sequence (Figure 8). Since such movements should be less energetically costly for peptides with core sequences that are not highly hydrophobic, they should be larger for LeuAla sequences than for all Leu sequences. This might contribute to the red shift observed for the pL_8A_8 and $p(LA)_8$ sequences relative to the pL_{16} sequence in DOPC, even if all three peptides form fully TM states.

Bilayer Response to Negative Mismatch: Effect Upon the Conformational Stability of Short TM Helices and Biological Implications

Natural membranes have nonpolar cores of about 30Å in width, and about 20 hydrophobic residues are believed to be required to span the bilayer. However, the latter number overlooks the ability of lipid bilayers to respond to mismatch. The observation in this report that short hydrophobic sequences have the ability to maintain a TM configuration in the presence of considerable negative mismatch can be most easily explained by mismatch-induced changes in bilayer structure. This explanation is consistent with studies showing that membrane proteins can maintain native structure and function to significant degree in the presence of mismatch[45–49]. Such studies suggest that forced hydrophobic matching occurs because TM proteins deform the surrounding lipid bilayer, which has flexible acyl chains, to adjust its hydrocarbon thickness to try to match the length of the hydrophobic surface of the protein[29,30,45,50,51]. Indeed, studies in model membranes have established that hydrophobic helix

length can affect local bilayer structure in this fashion when there is mismatch between the length of the hydrophobic sequence and the width of the hydrophobic segment of the bilayer[29,52].

On the other hand, some of the ability to tolerate mismatch is likely to involve adjustments in protein structure[29]. For example, when helices are especially long (i.e. under conditions of *positive* mismatch), changes in helix tilt might compensate for mismatch[29]. For single TM helices significant changes in tilt as a function of bilayer width have inferred indirectly[2], and directly observed for some sequences[22,32,53–56] although in other cases tilt changes have been reported to be rather small[40].

If the maximum amount of negative mismatch that can be tolerated is affected by the limits of lipid deformation then mechanical bilayer properties, which have already been proposed to affect function via changes in TM helix dynamics[57], could be a major factor in controlling the amount of mismatch that can be tolerated by short TM helices. Since membranes rich in cholesterol and sphingolipids are likely to be less easily deformed than those rich in unsaturated phospholipids, this could be of biological significance. Differential sorting of short and long TM helices to different membranes in eukaryotic cells (see Introduction), is thought to be due to the fact that the plasma membrane bilayer is significantly wider than that of the Golgi or endoplasmic reticulum[13,50]. This width difference might be due to a combination of differential content of cholesterol, differential lipid acyl chain saturation, or TM protein effects[50]. In any case, because these membranes also have different amounts of sphingolipids and cholesterol, they may differ in their ability to distort in response to mismatch, and this could also impact the dependence of sorting upon TM helix length.

Other Factors that May Alter Minimum TM Length In Vitro and In Vivo

In addition to average core hydrophobicity and flanking residue hydrophilicity, minimum TM length might be affected by several variables *in vivo*. One such variable examined in this report was the effect of a hydrophobicity gradient along the peptide sequence. We found very little difference between LeuAla sequences with uniform hydrophobicity and LeuAla sequences with a hydrophobicity gradient. This implies that it is not necessary to sacrifice TM stability in order to design a sequence with a hydrophobicity gradient. In contrast, a recent study has shown that the amphiphilicity of a sequence should have a very significant effect on TM stability[58]. Helix-helix interactions are another obvious variable that would affect the stability of the TM configurations. If there are favorable interactions in the TM state relative to the surface state, the TM state should be stabilized. (In this study, we used flanking sequences that minimize helix-helix interaction via electrostatic repulsions[20].) A third important variable, noted above, is the structure of the membrane lipids. In preliminary studies we have found that lipid headgroup structure can stabilize or destabilize TM insertion and thus alter minimum TM length (K. Shahidullah and E. London, unpublished observations). Finally, it should be noted that kinetic trapping during biosynthesis might alter minimum TM length *in vivo*. If, during biosynthesis, a short TM sequence is more stable within the translocon than in the lipid bilayer, it might be permanently trapped in the TM state after release from the translocon if surrounded by hydrophilic sequences that are too large to cross a lipid bilayer. For all these reasons, formation of stable or metastable TM helices with hydrophobic cores shorter than 11 residues long cannot be ruled out[3] .

MATERIALS AND METHODS

Materials

Peptides used in this study are listed in Table 1. These peptides were purchased from Anaspec Inc. (San Jose, CA). Peptides were purified via reverse-phase-HPLC using a C18 column with

2-proponal/water/0.5% v/v trifluoroacetic acid as mobile phase as described previously[35]. Peptide purity was confirmed using MALDI-TOF mass spectrometry (Proteomics Center, Stony Brook University). We estimated that final purity was on the order of 90% or better. After drying the HPLC fractions the peptides were stored in 1:1 (v/v) 2-proponal/water at 4 ºC. Peptide concentrations were measured by absorbance spectroscopy on a Beckman DU-650 spectrophotometer, using ε for Trp of 5560 $M^{-1}cm^{-1}$ at 280 nm. A series of 1,2-diacyl-*sn*-glycero-3-phosphocholines (phosphatidylcholines, PC): diC14:1Δ9cPC (dimyristoleoyl-PC, DMoPC); diC16:1Δ9cPC (dipalmitoleoyl-PC, DPoPC); diC18:1Δ9cPC (dioleoyl-PC, DOPC); diC20:1Δ11cPC (diecosenoyl-PC, DEiPC); diC22:1Δ13cPC (dierucoyl-PC, DEuPC) and diC24:1Δ15cPC (dinervonoyl-PC, DNPC) were purchased from Avanti Polar Lipids (Alabaster, AL). Concentrations of lipids purchased as liquid solutions were confirmed by dry weight. The lipids were stored in chloroform at −20ºC. 10-doxylnonadecane (10-DN) was custom synthesized by Molecular Probes (Eugene, OR). It was stored as a 6.1 mM stock solution in ethanol at −20 ºC.

Model Membrane Vesicle Preparation

Small unilamellar model membrane vesicles were prepared using the ethanol dilution method as previously described[2,22]. Peptides dissolved in 1:1 (v/v) 2-proponal/water and lipids dissolved in chloroform were mixed and dried under a stream of N_2 gas. Samples were then dried under high vacuum for 1h. The dried peptide/lipid samples were then dissolved in a minimum volume (10 μl) of ethanol and diluted to the desired final volume (typically 800 μl) using PBS (10mM sodium phosphate and 150mM NaCl, pH 7.0), with constant vortexing. Low and high pH samples were prepared using PBS (10mM sodium phosphate and 150mM NaCl) adjusted to the required pH using glacial acetic acid (pH 4.0) or NaOH (pH 9.0), respectively.

Multilamellar vesicles (MLV) for control experiments (Supplemental Figure 1) were prepared using PBS (10 mM sodium phosphate, 150 mM NaCl, pH 7.0) as described previously[59]. Dried peptide/lipid mixtures were dispersed in buffer at 70 °C for 15 min using a multi-tube vortexer, and then cooled to 25 °C. Samples were allowed to equilibrate for 30–60 min at room temperature before spectra were recorded.

Unless otherwise noted, for all model membrane samples final concentrations were 2 μM peptide and 500 μM lipid.

Fluorescence Measurements

Fluorescence data was obtained on SPEX τ2 Fluorolog spectrofluorometer operating in steady-state fluorescence mode at room temperature. Excitation slits of 2.5mm (4.5 nm band-pass) and emission slits of 5mm (9 nm band-pass) were used for all measurements. The fluorescence emission spectra were measured over the range 300–375 nm. Fluorescence from background samples containing lipid and buffer with no peptide were subtracted to calculate reported fluorescence values. All measurements were made at room temperature.

Acrylamide Quenching Measurements

To measure acrylamide quenching, fluorescence intensity and emission spectra were first measured in samples containing peptides incorporated into model membranes or background samples, prepared as described above. Then a 50 μl aliquot of acrylamide from a 4M stock solution dissolved in water was added. After a brief incubation (5 min), the fluorescence was remeasured. In these experiments, fluorescence intensity was measured using an excitation wavelength of 295 nm and emission wavelength of 340 nm. This excitation wavelength was chosen to reduce acrylamide absorbance (and the resulting inner-filter effect). Fluorescence intensity was corrected both for dilution from addition of acrylamide and due to the inner-filter

effect[33]. To determine emission λmax, Trp emission spectra in the presence of acrylamide were measured with an excitation wavelength of 280 nm, which gave stronger fluorescence intensity than with excitation at 295 nm despite the increased inner-filter effect due to acrylamide absorbance at 280 nm. Previous controls show that in these experiments the emission spectra λmax is not affected by this choice of excitation wavelength[33].

10-Doxylnonadecane Quenching Measurements

To measure quenching by 10-DN, the fluorescence of samples containing model membrane-incorporated peptide was compared to that in samples containing 10-DN. To prepare the later, samples were prepared as described above except that either 10% mol (for DOPC) or 12% mol (for DEuPC) of the lipid was replaced with an equivalent mol % of 10-DN. Fluorescence intensity was measured using an excitation wavelength of 280 nm and emission wavelength of 330 nm. The emission spectra were measured with excitation wavelength of 280 nm.

Calculation of Acrylamide/10-DN Quenching Ratio

The acrylamide/10-DN quenching ratio (Q-ratio) was used to estimate Trp depth in the bilayer. The ratio was calculated from the formula Q-ratio = $[(F_o/F_{acrylamide}) - 1]/ [(F_o/F_{10\text{-}DN}) - 1]$, where F_o is the fluorescence of a sample with no quencher present and $F_{acrylamide}$ and $F_{10\text{-}DN}$ are the fluorescence intensities in presence of acrylamide or 10-DN respectively. The Q-ratio varies inversely with depth of the Trp in the membrane[33].

Circular Dichroism Measurements

Circular dichroism (CD) spectra were recorded at room temperature using a JASCO J-715 CD spectrometer using 1 mm pathlength quartz cuvettes. Typically, final spectra were the average of 50 scans taken at a rate of 50 nm/min. All measurements were made with 2 μM peptide and 500 μM lipid. Estimation of α-helical content was done using DICHROWEB, a online server for secondary structure analyses from CD data[60]. Intensities in background samples (lipid without peptides) were subtracted before analysis of secondary structure.

Supplementary Material

Refer to Web version on PubMed Central for supplementary material.

Acknowledgements

† This work was supported by NIH grant GM48596.

References

1. Fujita K, Krishnakumar SS, Franco D, Paul AV, London E, Wimmer E. Membrane topography of the hydrophobic anchor sequence of poliovirus 3A and 3AB proteins and the functional effect of 3A/3AB membrane association upon RNA replication. Biochemistry 2007;46:5185–99. [PubMed: 17417822]
2. Ren J, Lew S, Wang J, London E. Control of the transmembrane orientation and interhelical interactions within membranes by hydrophobic helix length. Biochemistry 1999;38:5905–12. [PubMed: 10231543]
3. Adams GA, Rose JK. Structural requirements of a membrane-spanning domain for protein anchoring and cell surface transport. Cell 1985;41:1007–15. [PubMed: 3924407]
4. Jeong SY, Gaume B, Lee YJ, Hsu YT, Ryu SW, Yoon SH, Youle RJ. Bcl-x(L) sequesters its C-terminal membrane anchor in soluble, cytosolic homodimers. Embo J 2004;23:2146–55. [PubMed: 15131699]
5. Kienker PK, Qiu X, Slatin SL, Finkelstein A, Jakes KS. Transmembrane insertion of the colicin Ia hydrophobic hairpin. J Membr Biol 1997;157:27–37. [PubMed: 9141356]
6. Qiu XQ, Jakes KS, Kienker PK, Finkelstein A, Slatin SL. Major transmembrane movement associated with colicin Ia channel gating. J Gen Physiol 1996;107:313–28. [PubMed: 8868045]

7. Rosconi MP, London E. Topography of helices 5–7 in membrane-inserted diphtheria toxin T domain: identification and insertion boundaries of two hydrophobic sequences that do not form a stable transmembrane hairpin. J Biol Chem 2002;277:16517–27. [PubMed: 11859081]
8. Rosconi MP, Zhao G, London E. Analyzing Topography of Membrane-Inserted Diphtheria Toxin T Domain Using BODIPY-Streptavidin: At Low pH, Helices 8 and 9 Form a Transmembrane Hairpin but Helices 5–7 Form Stable Nonclassical Inserted Segments on the cis Side of the Bilayer. Biochemistry 2004;43:9127–39. [PubMed: 15248770]
9. Wattenberg B, Lithgow T. Targeting of C-terminal (tail)-anchored proteins: understanding how cytoplasmic activities are anchored to intracellular membranes. Traffic 2001;2:66–71. [PubMed: 11208169]
10. Ladokhin AS, Isas JM, Haigler HT, White SH. Determining the membrane topology of proteins: insertion pathway of a transmembrane helix of annexin 12. Biochemistry 2002;41:13617–26. [PubMed: 12427023]
11. Dalley JA, Bulleid NJ. The endoplasmic reticulum (ER) translocon can differentiate between hydrophobic sequences allowing signals for glycosylphosphatidylinositol anchor addition to be fully translocated into the ER lumen. J Biol Chem 2003;278:51749–57. [PubMed: 14530277]
12. Zhao G, London E. An amino acid “transmembrane tendency” scale that approaches the theoretical limit to accuracy for prediction of transmembrane helices: relationship to biological hydrophobicity. Protein Sci 2006;15:1987–2001. [PubMed: 16877712]
13. Bretscher MS, Munro S. Cholesterol and the Golgi apparatus. Science 1993;261:1280–1. [PubMed: 8362242]
14. Munro S. An investigation of the role of transmembrane domains in Golgi protein retention. Embo J 1995;14:4695–704. [PubMed: 7588599]
15. Webb RJ, East JM, Sharma RP, Lee AG. Hydrophobic mismatch and the incorporation of peptides into lipid bilayers: a possible mechanism for retention in the Golgi. Biochemistry 1998;37:673–9. [PubMed: 9425090]
16. Brandizzi F, Frangne N, Marc-Martin S, Hawes C, Neuhaus JM, Paris N. The destination for single-pass membrane proteins is influenced markedly by the length of the hydrophobic domain. Plant Cell 2002;14:1077–92. [PubMed: 12034898]
17. Karsten V, Hegde RS, Sinai AP, Yang M, Joiner KA. Transmembrane domain modulates sorting of membrane proteins in Toxoplasma gondii. J Biol Chem 2004;279:26052–7. [PubMed: 15056659]
18. Masibay AS, Balaji PV, Boeggeman EE, Qasba PK. Mutational analysis of the Golgi retention signal of bovine beta-1,4-galactosyltransferase. J Biol Chem 1993;268:9908–16. [PubMed: 8387508]
19. Caputo GA, London E. Cumulative effects of amino acid substitutions and hydrophobic mismatch upon the transmembrane stability and conformation of hydrophobic alpha-helices. Biochemistry 2003;42:3275–85. [PubMed: 12641459]
20. Lew S, Caputo GA, London E. The effect of interactions involving ionizable residues flanking membrane-inserted hydrophobic helices upon helix-helix interaction. Biochemistry 2003;42:10833–42. [PubMed: 12962508]
21. Lew S, Ren J, London E. The effects of polar and/or ionizable residues in the core and flanking regions of hydrophobic helices on transmembrane conformation and oligomerization. Biochemistry 2000;39:9632–40. [PubMed: 10933779]
22. Ren J, Lew S, Wang Z, London E. Transmembrane orientation of hydrophobic alpha-helices is regulated both by the relationship of helix length to bilayer thickness and by the cholesterol concentration. Biochemistry 1997;36:10213–20. [PubMed: 9254619]
23. Aisenbrey C, Goormaghtigh E, Ruysschaert JM, Bechinger B. Translocation of amino acyl residues from the membrane interface to the hydrophobic core: thermodynamic model and experimental analysis using ATR-FTIR spectroscopy. Mol Membr Biol 2006;23:363–74. [PubMed: 16923729]
24. Bechinger B. Towards membrane protein design: pH-sensitive topology of histidine-containing polypeptides. J Mol Biol 1996;263:768–75. [PubMed: 8947574]
25. Mall S, Broadbridge R, Sharma RP, Lee AG, East JM. Effects of aromatic residues at the ends of transmembrane alpha-helices on helix interactions with lipid bilayers. Biochemistry 2000;39:2071–8. [PubMed: 10684657]

26. Hunt JF, Rath P, Rothschild KJ, Engelman DM. Spontaneous, pH-dependent membrane insertion of a transbilayer alpha-helix. Biochemistry 1997;36:15177–92. [PubMed: 9398245]
27. Killian JA, Nyholm TK. Peptides in lipid bilayers: the power of simple models. Curr Opin Struct Biol 2006;16:473–9. [PubMed: 16828281]
28. van Duyl BY, Meeldijk H, Verkleij AJ, Rijkers DT, Chupin V, de Kruijff B, Killian JA. A synergistic effect between cholesterol and tryptophan-flanked transmembrane helices modulates membrane curvature. Biochemistry 2005;44:4526–32. [PubMed: 15766283]
29. Killian JA. Hydrophobic mismatch between proteins and lipids in membranes. Biochim Biophys Acta 1998;1376:401–15. [PubMed: 9805000]
30. Goforth RL, Chi AK, Greathouse DV, Providence LL, Koeppe RE 2nd, Andersen OS. Hydrophobic coupling of lipid bilayer energetics to channel function. J Gen Physiol 2003;121:477–93. [PubMed: 12719487]
31. Liu F, Lewis RN, Hodges RS, McElhaney RN. Effect of variations in the structure of a polyleucine-based alpha-helical transmembrane peptide on its interaction with phosphatidylethanolamine Bilayers. Biophys J 2004;87:2470–82. [PubMed: 15454444]
32. Duong-Ly KC, Nanda V, Degrado WF, Howard KP. The conformation of the pore region of the M2 proton channel depends on lipid bilayer environment. Protein Sci 2005;14:856–61. [PubMed: 15741338]
33. Caputo GA, London E. Using a novel dual fluorescence quenching assay for measurement of tryptophan depth within lipid bilayers to determine hydrophobic alpha-helix locations within membranes. Biochemistry 2003;42:3265–74. [PubMed: 12641458]
34. Caputo GA, London E. Position and ionization state of Asp in the core of membrane-inserted alpha helices control both the equilibrium between transmembrane and nontransmembrane helix topography and transmembrane helix positioning. Biochemistry 2004;43:8794–806. [PubMed: 15236588]
35. Lew S, London E. Simple procedure for reversed-phase high-performance liquid chromatographic purification of long hydrophobic peptides that form transmembrane helices. Anal Biochem 1997;251:113–6. [PubMed: 9300091]
36. Zhang YP, Lewis RN, Henry GD, Sykes BD, Hodges RS, McElhaney RN. Peptide models of helical hydrophobic transmembrane segments of membrane proteins. 1. Studies of the conformation, intrabilayer orientation, and amide hydrogen exchangeability of Ac-K2-(LA)12-K2-amide. Biochemistry 1995;34:2348–61. [PubMed: 7857945]
37. Killian JA, von Heijne G. How proteins adapt to a membrane-water interface. Trends Biochem Sci 2000;25:429–34. [PubMed: 10973056]
38. Wimley WC, White SH. Experimentally determined hydrophobicity scale for proteins at membrane interfaces. Nat Struct Biol 1996;3:842–8. [PubMed: 8836100]
39. Hessa T, Kim H, Bihlmaier K, Lundin C, Boekel J, Andersson H, Nilsson I, White SH, von Heijne G. Recognition of transmembrane helices by the endoplasmic reticulum translocon. Nature 2005;433:377–81. [PubMed: 15674282]
40. Ozdirekcan S, Rijkers DT, Liskamp RM, Killian JA. Influence of flanking residues on tilt and rotation angles of transmembrane peptides in lipid bilayers. A solid-state 2H NMR study. Biochemistry 2005;44:1004–12. [PubMed: 15654757]
41. Davis JH, Clare DM, Hodges RS, Bloom M. Interaction of a Synthetic Amphiphilic Polypeptide and Lipids in a Bilayer Structure. Biochemistry 1983;22:5298–5305.
42. Hammond K, Caputo GA, London E. Interaction of the membrane-inserted diphtheria toxin T domain with peptides and its possible implications for chaperone-like T domain behavior. Biochemistry 2002;41:3243–53. [PubMed: 11863463]
43. Bechinger B. Membrane insertion and orientation of polyalanine peptides: a (15)N solid-state NMR spectroscopy investigation. Biophys J 2001;81:2251–6. [PubMed: 11566795]
44. Lewis RN, Zhang YP, Hodges RS, Subczynski WK, Kusumi A, Flach CR, Mendelsohn R, McElhaney RN. A polyalanine-based peptide cannot form a stable transmembrane alpha-helix in fully hydrated phospholipid bilayers. Biochemistry 2001;40:12103–11. [PubMed: 11580285]
45. Caffrey M, Feigenson GW. Fluorescence quenching in model membranes. 3. Relationship between calcium adenosinetriphosphatase enzyme activity and the affinity of the protein for

phosphatidylcholines with different acyl chain characteristics. Biochemistry 1981;20:1949–61. [PubMed: 6452902]

46. Dumas F, Tocanne JF, Leblanc G, Lebrun MC. Consequences of hydrophobic mismatch between lipids and melibiose permease on melibiose transport. Biochemistry 2000;39:4846–54. [PubMed: 10769142]
47. Pilot JD, East JM, Lee AG. Effects of bilayer thickness on the activity of diacylglycerol kinase of Escherichia coli. Biochemistry 2001;40:8188–95. [PubMed: 11444964]
48. Johannsson A, Smith GA, Metcalfe JC. The effect of bilayer thickness on the activity of (Na+ + K +)-ATPase. Biochim Biophys Acta 1981;641:416–21. [PubMed: 6111345]
49. Johannsson A, Keightley CA, Smith GA, Richards CD, Hesketh TR, Metcalfe JC. The effect of bilayer thickness and n-alkanes on the activity of the (Ca2+ + Mg2+)-dependent ATPase of sarcoplasmic reticulum. J Biol Chem 1981;256:1643–50. [PubMed: 6109722]
50. Mitra K, Ubarretxena-Belandia I, Taguchi T, Warren G, Engelman DM. Modulation of the bilayer thickness of exocytic pathway membranes by membrane proteins rather than cholesterol. Proc Natl Acad Sci U S A 2004;101:4083–8. [PubMed: 15016920]
51. Mouritsen OG, Bloom M. Mattress model of lipid-protein interactions in membranes. Biophys J 1984;46:141–53. [PubMed: 6478029]
52. de Planque MR, Boots JW, Rijkers DT, Liskamp RM, Greathouse DV, Killian JA. The effects of hydrophobic mismatch between phosphatidylcholine bilayers and transmembrane alpha-helical peptides depend on the nature of interfacially exposed aromatic and charged residues. Biochemistry 2002;41:8396–404. [PubMed: 12081488]
53. Koehorst RB, Spruijt RB, Vergeldt FJ, Hemminga MA. Lipid bilayer topology of the transmembrane alpha-helix of M13 Major coat protein and bilayer polarity profile by site-directed fluorescence spectroscopy. Biophys J 2004;87:1445–55. [PubMed: 15345527]
54. Kovacs FA, Denny JK, Song Z, Quine JR, Cross TA. Helix tilt of the M2 transmembrane peptide from influenza A virus: an intrinsic property. J Mol Biol 2000;295:117–25. [PubMed: 10623512]
55. Park SH, Mrse AA, Nevzorov AA, Mesleh MF, Oblatt-Montal M, Montal M, Opella SJ. Three-dimensional structure of the channel-forming trans-membrane domain of virus protein “u” (Vpu) from HIV-1. J Mol Biol 2003;333:409–24. [PubMed: 14529626]
56. Park SH, Opella SJ. Tilt angle of a trans-membrane helix is determined by hydrophobic mismatch. J Mol Biol 2005;350:310–8. [PubMed: 15936031]
57. Grinthal A, Guidotti G. Bilayer mechanical properties regulate the transmembrane helix mobility and enzymatic state of CD39. Biochemistry 2007;46:279–90. [PubMed: 17198399]
58. Fernandez-Vidal M, Jayasinghe S, Ladokhin AS, White SH. Folding amphipathic helices into membranes: amphiphilicity trumps hydrophobicity. J Mol Biol 2007;370:459–70. [PubMed: 17532340]
59. Xu X, London E. The effect of sterol structure on membrane lipid domains reveals how cholesterol can induce lipid domain formation. Biochemistry 2000;39:843–9. [PubMed: 10653627]
60. Whitmore L, Wallace BA. DICHROWEB, an online server for protein secondary structure analyses from circular dichroism spectroscopic data. Nucleic Acids Res 2004;32:W668–73. [PubMed: 15215473]

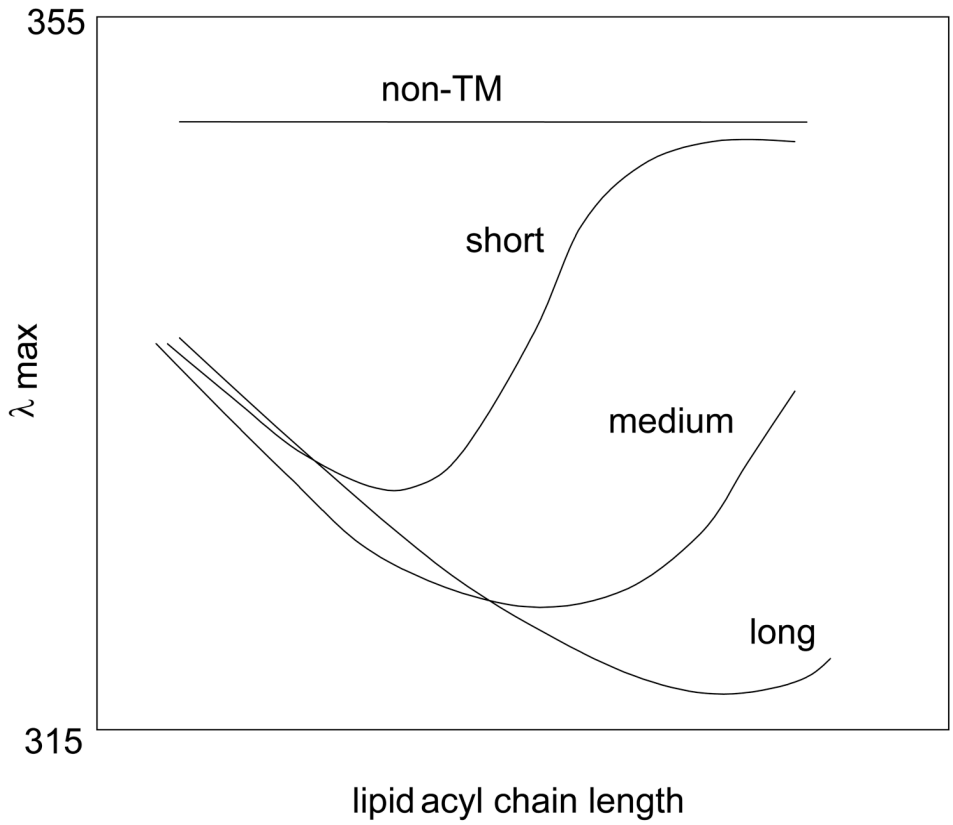

Figure 1.
Schematic representation of the dependence of Trp λmax upon lipid acyl chain length for hydrophobic peptides with different lengths and tendencies to form a TM topography[2,19,21,22,34]. Short, medium, and long refer to the length of hydrophobic sequences sufficiently hydrophobic to form TM sequences in the absence of negative mismatch. Non-TM shows the behavior of a sequence insufficiently hydrophobic to form a TM state at any bilayer width.

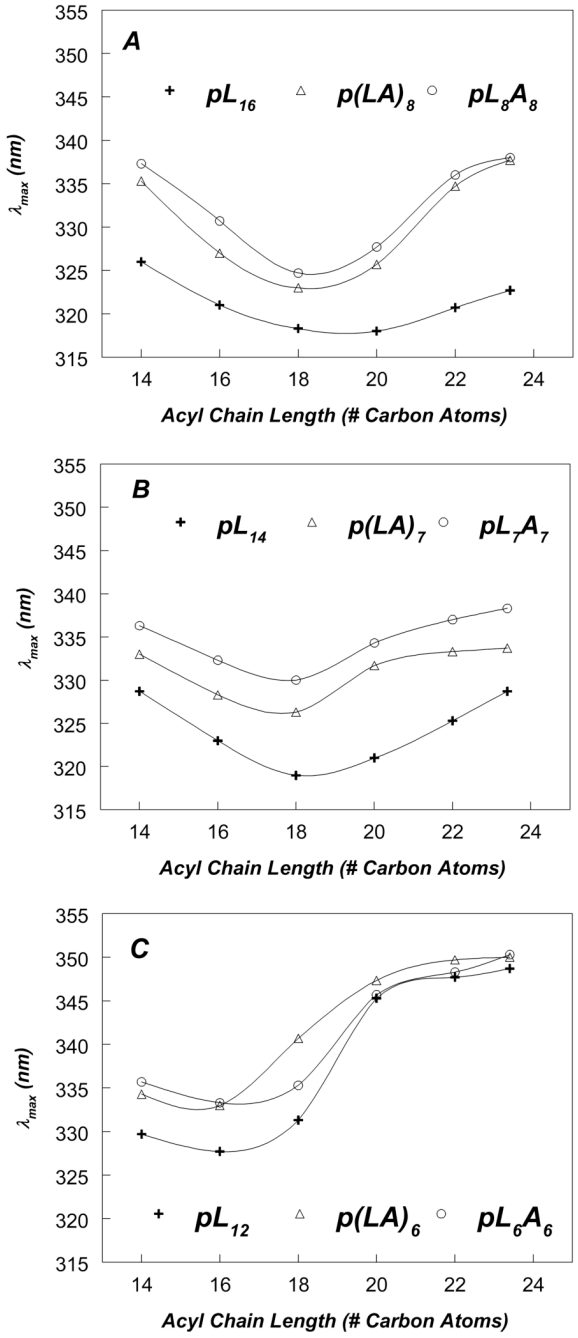

Figure 2.

Effect of lipid acyl chain length on Trp emission λmax of pLeu and pLeuAla peptides of varying lengths incorporated into phosphatidylcholine vesicles at pH 7.0. (A) pLeu and pLeuAla peptides with 17-residue hydrophobic core. (B) pLeu and pLeuAla peptides with 15-residue hydrophobic core. (C) pLeu and pLeuAla peptides with 13-residue hydrophobic core. Samples contained 2 μM peptide incorporated into 500 μM lipid dispersed in PBS at pH 7.0. The average λmax values from a minimum of triplicate samples are shown. Generally, λmax in individual samples was reproducible to within ± 1 nm of the average value.

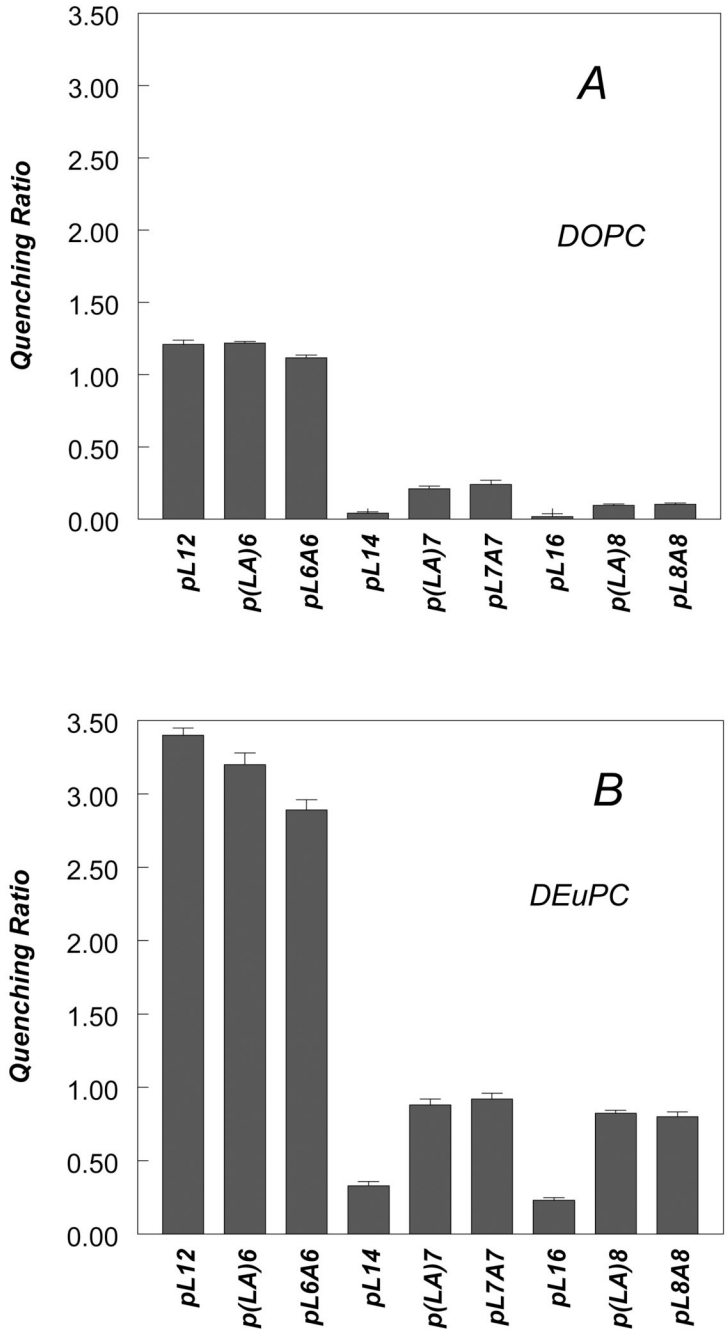

Figure 3.

Quenching ratios for pLeu and pLeuAla peptides of varying lengths incorporated into DOPC and DEuPC vesicles at pH 7.0. (A) Quenching ratio of peptides in DOPC vesicles at pH 7.0. (B) Quenching ratio of peptides in DEuPC vesicles at pH 7.0. Samples contained 2 μM peptide incorporated into 500 μM lipid dispersed in PBS at pH 7.0. Average and standard deviation from a minimum of 3 samples are shown.

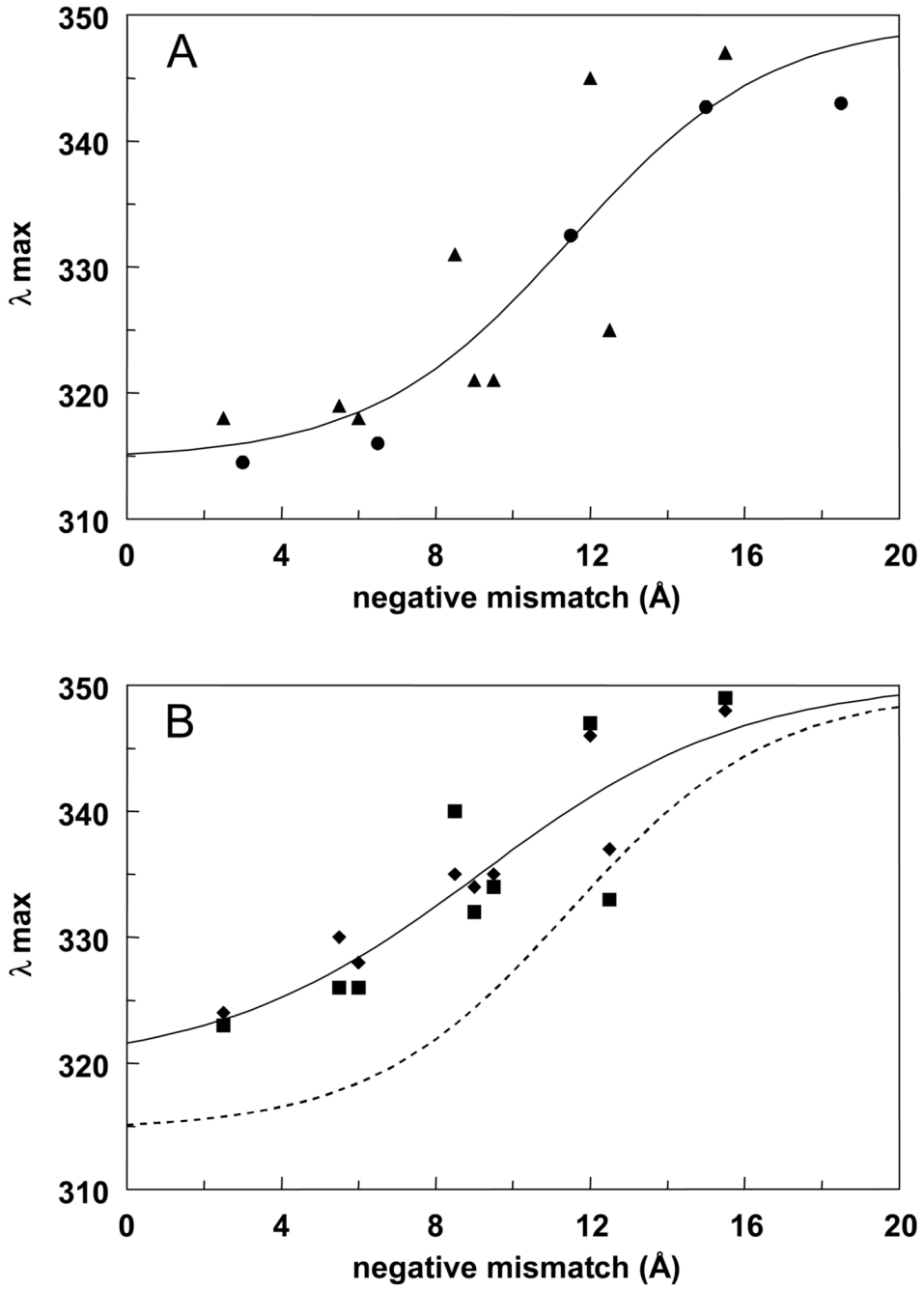

Figure 4.

Dependence of Trp λmax upon the degree of negative mismatch between hydrophobic segment length and bilayer width. (A) pL peptides. Data from Figure 2 (triangles) and for pL_{10} and pL_{18} peptides from Ren *et al*, 1999 2 (circles) in DOPC, DEiPC and DEuPC vesicles. Solid line shows sigmoidal fit to the data, with a limiting λmax of 350 nm at infinite negative mismatch. (SlideWrite program, Advanced Graphics Software, Encinitas, CA). (B) pLA peptides. Data derived from Figure 2 is shown for p(LA)n (squares) and pLnAn (diamonds) in DOPC, DEiPC and DEuPC vesicles. Solid line shows sigmoidal fit with a λmax of 350 nm at infinite negative mismatch. Dashed line shows the sigmoidal fit from panel A. for

comparison. Negative mismatch was calculated from the formula: bilayer width^2 - hydrophobic sequence length =(1.5 Å)(number of hydrophobic residues).

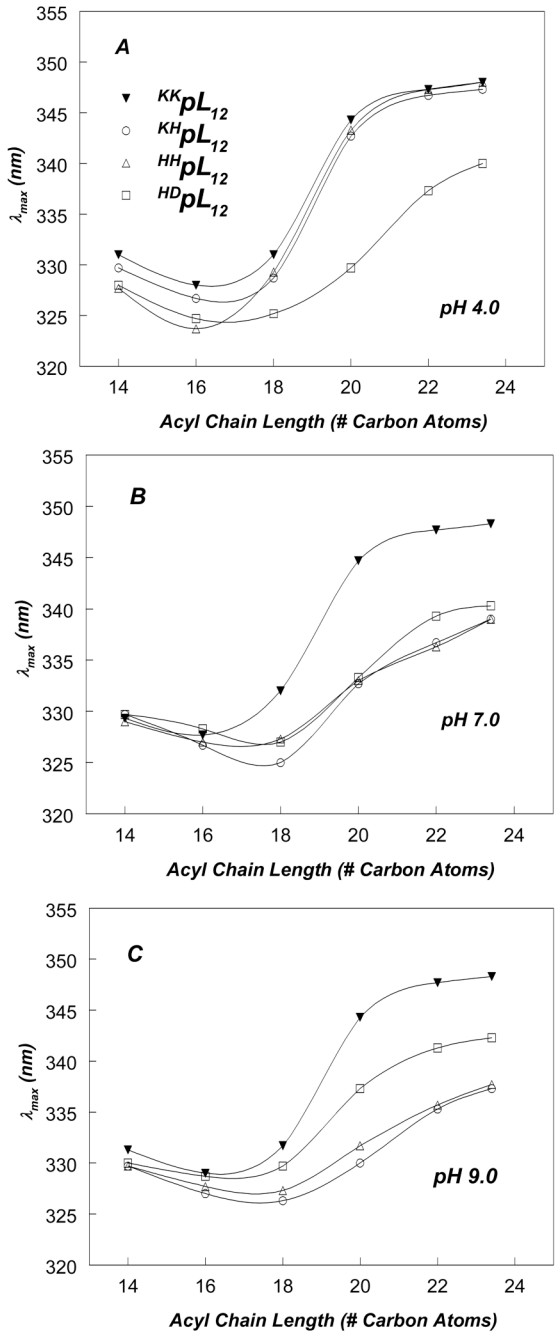

Figure 5.

Effect of lipid acyl chain length on Trp emission λmax for pLeu peptides with varying flanking residues incorporated into phosphatidylcholine vesicles at: (A) pH 4.0; (B) pH 7.0 (C); pH 9.0. Symbols: (filled triangles) $^{KK}pL_{12}$, (open circles) $KHpL_{12}$, (open triangles) $HHpL_{12}$, and (open squares) $^{HD}pL_{12}$. The samples contained 2 μM peptide incorporated into 500 μM lipid dispersed in pH-adjusted PBS. Average values from 3 samples are shown.

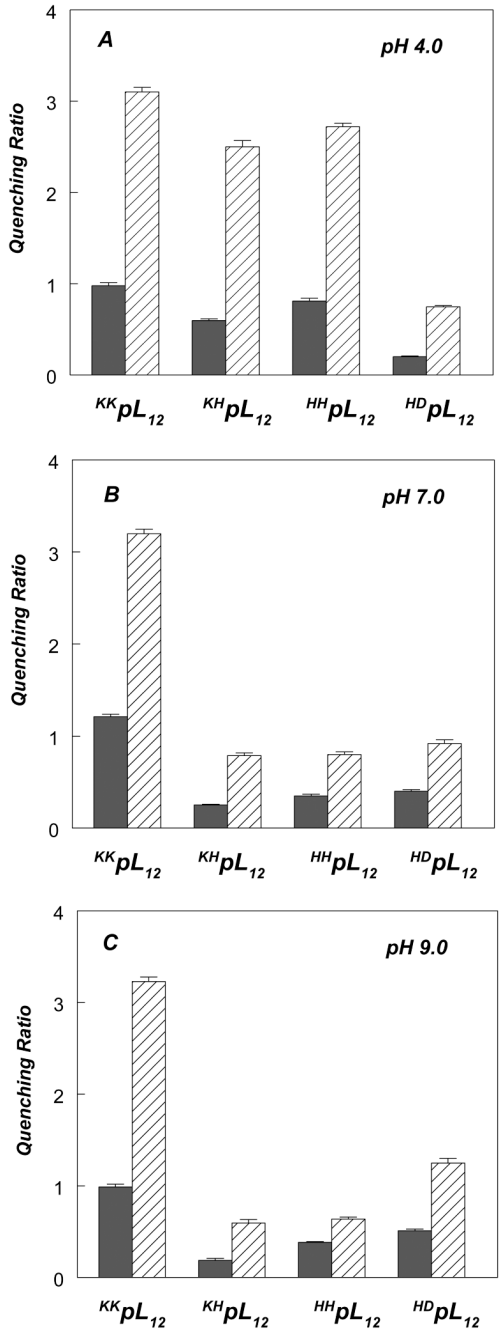

Figure 6.

Quenching ratios for pL_{12} peptides with varying flanking residues incorporated into DOPC (filled bars) or DEuPC (striped bars) vesicles. (A) Q-ratios at pH 4.0, (B) Q-ratios at pH 7.0, (C) Q-ratios at pH 9.0. Samples contained 2 μM peptide incorporated into 500 μM lipid dispersed in PBS of different pH. Average and standard deviation for triplicates are shown.

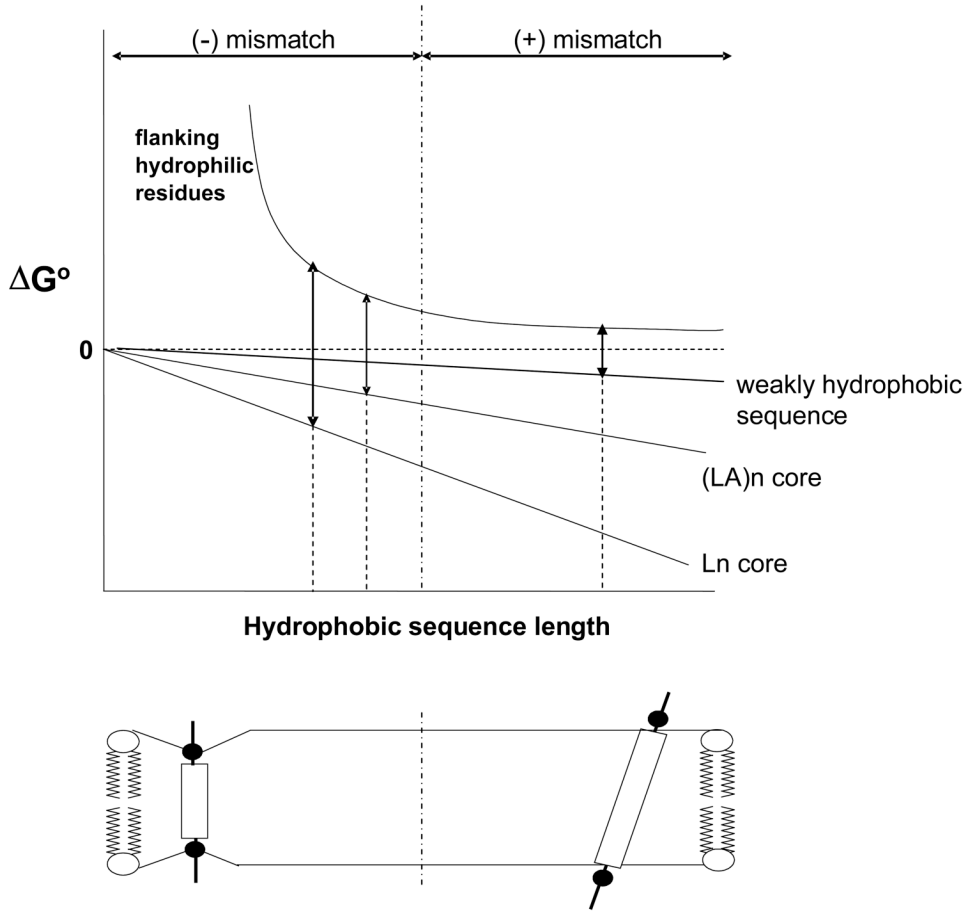

Figure 7.

Schematic illustration of the energetics of TM helix stability as a function of hydrophobic sequence length. ΔG^o is the free energy of the TM configuration relative to that of the non-TM configuration. The energetic contributions of the hydrophobic core and flanking hydrophilic sequences are shown as separate components. The vertical dashed-and-dotted line represents the boundary between negative and positive mismatch. The TM configuration of the helix is shown below the graph under conditions of negative (left) and positive (right) mismatch. The double arrows are shown at the minimum TM length (given by the intercept of the dashed lines and x-axis), which is the point at which ΔG^o for membrane burial of the hydrophobic core (down arrow) = ΔG^o for membrane burial of the flanking hydrophilic residues (up arrow). Notice that for a weakly hydrophobic sequence the minimum TM length would fall in the region of positive mismatch and would be very sensitive to the hydrophobicity of the peptide core.

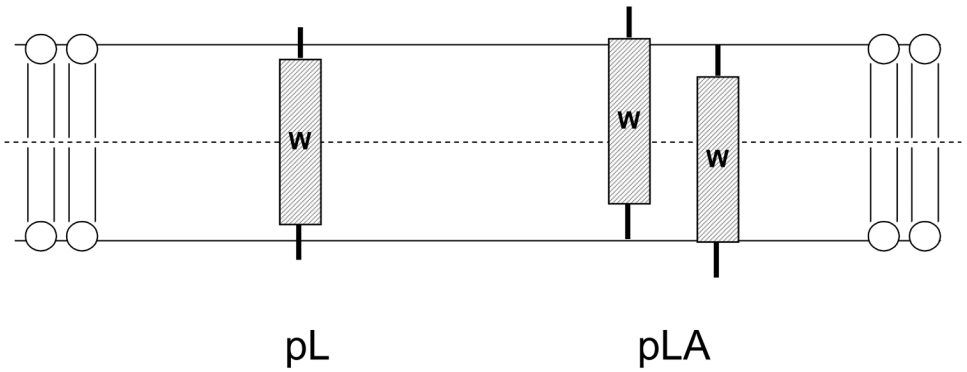

Figure 8.
Schematic illustration of possible difference in anchoring of the TM state for pL (left) and pLA (right) peptides. Trp is shown as a W. Note that the average Trp distance from the bilayer center is greater for the pLA peptides even though average Trp location is at the bilayer center in both cases. Distortion in bilayer structure induced by peptides is not shown

Table 1

List of Peptides Used in this Study.

Peptide	Sequence
$pL_{12} = ({}^{KK}pL_{12})$	Ac-(= acetyl)-$K_2GL_6WL_6K_2A$-NH_2
pL_{14}	Ac-$K_2GL_7WL_7K_2A$-NH_2
pL_{16}	Ac-$K_2GL_8WL_8K_2A$-NH_2
$p(LA)_6$	Ac-$K_2G(LA)_3W(LA)_3K_2A$-NH_2
$p(LA)_7$	Ac-$K_2G(LA)_3LWA(LA)_3K_2A$-NH_2
$p(LA)_8$	Ac-$K_2G(LA)_4W(LA)_4K_2A$-NH_2
pL_6A_6	Ac-$K_2GL_6WA_6K_2A$-NH_2
pL_7A_7	Ac-$K_2GL_7WA_7K_2A$-NH_2
pL_8A_8	Ac-$K_2GL_8WA_8K_2A$-NH_2
${}^{KH}pL_{12}$	Ac-$KHGL_6WL_6HKA$-NH_2
${}^{HH}pL_{12}$	Ac-$H_2L_6WL_6H_2$-NH_2
${}^{HD}pL_{12}$	Ac-$HDGL_6WL_6DHA$-NH_2

Table 2

Quencher-Induced Shifts in Trp Emission λmax for Membrane-Inserted Peptides in DOPC and DEuPC Bilayers

Peptide	Lipid	λmax (nm)[a]	λmax (nm) (acrylamide)	λmax (nm) (10-DN)	|Δλmax| (nm)[b]	Likely Helix Configuration [c]
pL_{16}	DOPC	318	319	318	1	TM
	DEuPC	321	321	320	1	TM
$p(LA)_8$	DOPC	323	322	324	2	TM
	DEuPC	334	333	336	3	Mostly non-TM
pL_8A_8	DOPC	324	324	325	1	TM
	DEuPC	335	335	339	4	Mostly non-TM
pL_{14}	DOPC	319	320	320	0	TM
	DEuPC	325	325	328	3	Mostly TM
$p(LA)_7$	DOPC	326	323	329	6	TM + non-TM
	DEuPC	333	333	337	4	Mostly non-TM
pL_7A_7	DOPC	330	326	333	7	TM + non-TM
	DEuPC	337	338	342	4	Mostly non-TM
pL_{12}	DOPC	331	329	339	10	TM + non-TM
	DEuPC	347	347	349	2	non-TM
$p(LA)_6$	DOPC	340	337	348	11	TM + non-TM
	DEuPC	349	347	349	2	non-TM
pL_6A_6	DOPC	335	330	344	13	TM + non-TM
	DEuPC	348	347	349	2	non-TM

[a] Reported λmax values are averages from three to six samples. The values were generally reproducible within ± 1nm. The λmax values have been rounded to whole numbers.

[b] δλmax is the absolute value of difference between λmax in the presence of acrylamide and λmax in the presence 10-DN.

[c] Likely helix configuration is derived from the absolute values of λmax in the absence of quencher combined with whether λmax shifts in the presence of quencher indicate more than one configuration is significantly populated.

Table 3

Quencher-Induced Shifts in Trp Emission λmax for Membrane-Inserted Peptides in DOPC and DEuPC Bilayers: Peptides with Different Hydrophilic Flanking Residues.

Peptide	pH	Lipid	λmax (nm)[a]	λmax (nm) (acrylamide)	λmax (nm) (10-DN)	|Δλmax| (nm)[b]
$^{KK}pL_{12}$	4	DOPC DEuPC	330 347	328 347	339 349	11 2
$^{KH}pL_{12}$	4	DOPC DEuPC	329 347	328 346	335 348	7 2
$^{HH}pL_{12}$	4	DOPC DEuPC	329 347	326 346	341 348	15 2
$^{HD}pL_{12}$	4	DOPC DEuPC	325 337	324 336	325 339	1 3
$^{KK}pL_{12}$	7	DOPC DEuPC	331 347	329 347	339 348	10 1
$^{KH}pL_{12}$	7	DOPC DEuPC	325 337	325 335	326 340	1 5
$^{HH}pL_{12}$	7	DOPC DEuPC	327 337	327 333	329 337	2 4
$^{HD}pL_{12}$	7	DOPC DEuPC	327 339	327 339	327 342	0 3
$^{KK}pL_{12}$	9	DOPC DEuPC	331 347	328 347	340 349	12 2
$^{KH}pL_{12}$	9	DOPC DEuPC	325 335	325 333	326 338	1 5
$^{HH}pL_{12}$	9	DOPC DEuPC	327 336	327 332	329 337	2 5
$^{HD}pL_{12}$	9	DOPC DEuPC	330 341	329 339	333 341	4 2

[a] Reported λmax values are averages from three samples. The values were generally reproducible within ± 1nm. The λmax values have been rounded to whole numbers.

[b] Δλmax is the absolute value of difference between λmax in the presence of acrylamide and λmax in the presence 10-DN